# Noisy one-way quantum computations: The role of correlations

Rafael Chaves[1,2,3,*] and Fernando de Melo[4,3,†]

[1]*ICFO-Institut de Ciencies Fotoniques, Mediterranean Technology Park, 08860 Castelldefels (Barcelona), España*

[2]*Instituto de Física, Universidade Federal do Rio de Janeiro, Rio de Janeiro, Brasil*

[3]*Physikalisches Institut der Albert–Ludwigs–Universität, Freiburg, Deutschland*

[4]*Instituut voor Theoretische Fysica, Katholieke Universiteit Leuven, Leuven, België*

(Received 13 April 2011; published 18 August 2011)

A scheme to evaluate computation fidelities within the one-way model is developed and explored to understand the role of correlations in the quality of noisy quantum computations. The formalism is promptly applied to many computation instances and unveils that a higher amount of entanglement in the noisy resource state does not necessarily imply a better computation.

DOI: 10.1103/PhysRevA.84.022324 PACS number(s): 03.67.Ac, 03.65.Yz

## I. INTRODUCTION

Since the advent of quantum computation [1], entanglement, a clear-cut quantum mechanical feature, is commonly believed the key resource behind it. Not surprisingly, the importance of correlations for quantum computations has been a much-debated subject. For *pure* state quantum computations certainly some entanglement is necessary if the quantum protocol is not to be efficiently simulated by classical means [2,3]. However, entanglement is only a necessary but not sufficient condition for an exponential gain of quantum computations over classical ones. There are quantum protocols that despite producing highly entangled states can still be efficiently simulated classically [2,4].

The scenario for *mixed* state quantum computations is far more subtle [2]. A model for mixed-state quantum computation introduced in [5], in which the input state consists of a single qubit in a pure-state and all the others in a uniform incoherent sum of classical alternatives, and therefore it is not entangled, offers an exponential speed-up to problems that are believed intractable by classical computers [6]. Also, room-temperature NMR implementations of quantum information tasks [7], which employ a rather noisy state where entanglement is known not to be present [8], seem to still present gain over classical computations [9]. Nevertheless, in these cases generation of entanglement during the computation itself cannot be ruled out [6]. A definitive statement about the influence of entanglement is thus challenging.

A clean investigation of the entanglement role in noisy quantum computations is however possible within the one-way model [10]. In this model local (projective) measurements on a highly entangled resource state are responsible for input preparation, the required computation, and final readout. No entanglement is created during the computation. We thus have a clear distinction between the entanglement creation and its use as a resource.

Employing this model of computation, we address here still another facet of the entanglement role in noisy quantum computations: How does the noise affecting the entangled resource state impact on the "quality" (fidelity) of the computation? Does a more entangled resource state always empower better computations? Or in more practical terms, should one always try to minimize the influence of the environment over the entanglement such as to maximize the fidelity of a computation? To answer in the negative to these questions, we derive an expression for the fidelity of any one-way computation when the resource state undergoes various types of decoherence. Our results extend to noisy computations the assertion [11] that a too entangled state is not always advantageous for a measurement based quantum computation.

This article is organized as follows: In Sec. II we briefly review the one-way model for quantum computations. In Sec. III we discuss the effects of various models of decoherence on one-way computations and derive the expression for the fidelity in such cases. In Sec. IV we apply the developed formalism to various computation instances, showing that a higher amount of entanglement in the noisy resource state does not necessarily imply better computations. In particular, we obtain that some instances of the Deutsch-Jozsa [12] algorithm, which in the circuit model of quantum computation generically create entangled states [13], within the one-way framework require no entanglement for their execution. In Sec. IV D we analyze the effects of decoherence in the ancilla-driven quantum computation proposed in Ref. [14]. In Sec. V we summarize our results and draw some conclusions.

## II. ONE-WAY MODEL OF QUANTUM COMPUTATION

In the one-way model [10] all the interactions between qubits and local unitary transformations needed by the protocol are exchanged by a prior entanglement in a graph state and the possibility to make adaptive local measurements. A graph state is defined by a set of vertices $\mathcal{V}$ and a collection of edges $\mathcal{E}$. In each vertex $i$ sits a qubit ($\mathcal{H}_2$) initialized in a state $|+_i\rangle = (|0_i\rangle + |1_i\rangle)/\sqrt{2}$, and an edge represents an interaction between vertices $\{i,j\}$ given by $\mathrm{CZ}_{ij} = |0_i\rangle\langle 0_i| \otimes \mathbb{1}_j + |1_i\rangle\langle 1_i| \otimes Z_j$. Hereafter $\{\mathbb{1}, X, Y, Z\}$ represents the usual $\{\sigma_0, \sigma_1, \sigma_2, \sigma_3\}$ Pauli matrices. The $N$-qubit graph state is then

$$|G_{(\mathcal{V},\mathcal{E})}\rangle = \prod_{\{i,j\}\in\mathcal{E}} \mathrm{CZ}_{ij} |+_k\rangle^{\otimes k\in\mathcal{V}}. \quad (1)$$

Starting with a $N$-qubit graph state, an one-way computation is carried out by measuring $M$ qubits and the remaining

*rafael.chaves@icfo.es

†fnando.demelo@gmail.com

 

$N-M$ qubits encode the protocol answer. The algorithm is then defined by a triple $\{\theta_i,\alpha_i,s_i\}$, with instructions on the measurement basis $|M_{k_i}^{s_i}(\theta_i,\alpha_i)\rangle$ for the $i$th qubit. Here

$$\begin{aligned}\left|M_{0_i}^{s_i}(\theta_i,\alpha_i)\right\rangle &= \cos\frac{\alpha_i}{2}|0\rangle + \sin\frac{\alpha_i}{2}\, e^{-i(-1)^{s_i}\theta_i}|1\rangle \\ \left|M_{1_i}^{s_i}(\theta_i,\alpha_i)\right\rangle &= \sin\frac{\alpha_i}{2}|0\rangle - \cos\frac{\alpha_i}{2}\, e^{-i(-1)^{s_i}\theta_i}|1\rangle\end{aligned} \tag{2}$$

with $s_i \equiv s_i(\vec{k}) = s_i(k_1,\ldots,k_M) \in \{0,1\}$ the adaptation parameter that depends on the outcome $k_j \in \{0,1\}$ of previous measurements and implicity on the algorithm being considered (hereafter, the notation $\vec{x}$ represents the M-tuple $x_1,\ldots,x_M$). The need for adaptations stems from the requirement of turning every computation deterministic, despite the intrinsic randomness associated with each quantum measurement. Adaptations introduce a temporal order for the measurements, and thus classical correlations other than those already present in the initial state. The only two instances of $\alpha_i$ necessary for all computations are $\alpha_i = 0$, for measurements along the $z$ direction, and $\alpha_i = \pi/2$, for measurements in the $x$-$y$ plane (equator) of the Bloch sphere. The measurements are nonadaptive when the basis is given by the Pauli operator $\{X,Y,Z\}$ eigenvectors, and possibly adaptive otherwise. Lastly, the desired answer is given aside some local unitary transformations, final by-products ($B$) of the computation, determined by the classical outcomes $\vec{k}$ of all measured qubits. These by-products can be dealt with by classical postprocessing.

Once a computation to be performed on a graph state $|G_{(\mathcal{V},\mathcal{E})}\rangle$ is defined, the $M$ qubits to be measured can be immediately written in their measurement basis (adaptations included) which elicits the answer

$$|G_{(\mathcal{V},\mathcal{E})}\rangle = \frac{1}{2^{\frac{M}{2}}}\sum_{\vec{k}}\bigotimes_{i=1}^{M}\left|M_{k_i}^{s_i}(\theta_i,\alpha_i)\right\rangle|A_{\vec{k}}(\vec{\theta},\vec{\alpha})\rangle, \tag{3}$$

with $|A_{\vec{k}}(\vec{\theta},\vec{\alpha})\rangle = B_{\vec{k}}|A_{\vec{0}}(\vec{\theta},\vec{\alpha})\rangle$, and $|A_{\vec{0}}(\vec{\theta},\vec{\alpha})\rangle$ the desired answer without the by-products. The latter, in turn, can be expressed as local unitaries

$$B_{\vec{k}} = \bigotimes_{i=N-M+1}^{N}(-1)^{f_{i,Sig}(\vec{k})}X_i^{f_{i,X}(\vec{k})}Z_i^{f_{i,Z}(\vec{k})}, \tag{4}$$

with $f_{Sig}$, $f_X$, and $f_Z$ Boolean functions of the outcomes $\vec{k}$ defined by the protocol at hand. In a noise-free computation, the sign Boolean function $f_{\mathrm{Sig}}$ only introduces a global phase on each answer and is then of no importance. However, under the action of the environment, some of the answers will be mixed, and this phase then becomes a relative one. As such, it cannot be neglected. It is important to notice that out of $2^M$ possible measurement outcomes in a given protocol, only $4^{N-M}$ of them possibly lead to different answers (modulo a global phase), meaning that in general many answers are the same.

## III. FIDELITY OF NOISY ONE-WAY QUANTUM COMPUTATIONS

Once the hardware (graph state) and algorithm (measurement basis + possible adaptations) are defined, we want to gauge how the quality of a computation decays due to different noisy environments and how this is related to the decay of the initial entanglement resource.

The standard measure for the computation quality is the output fidelity $\mathcal{F}$ [1,15–20]. This measure compares the desired state $|\Psi_{\mathrm{out}}\rangle$ with the actually obtained one $\varrho_{\mathrm{out}}$, giving $\mathcal{F}(|\Psi_{\mathrm{out}}\rangle,\varrho_{\mathrm{out}}) := \langle\Psi_{\mathrm{out}}|\varrho_{\mathrm{out}}|\Psi_{\mathrm{out}}\rangle$. The fidelity measure is also used to define the error threshold for quantum computations [21,22].

In what follows, we consider that each qubit of the initial graph state is individually coupled to its own thermal environment. A great variety of single-qubit open dynamics is encompassed by the map [23]

$$\begin{aligned}\Lambda_k(\bullet) = &\sum_{j=0}^{3}\lambda_j^k(t)\,\sigma_j\bullet\sigma_j + \mu^k(t) \\ &\times[\sigma_3\bullet\sigma_0 + \sigma_0\bullet\sigma_3 - i\sigma_1\bullet\sigma_2 + i\sigma_2\bullet\sigma_1]\end{aligned} \tag{5}$$

with

$$\begin{aligned}\lambda_0^k(t) &= \frac{1+2e^{-C_kt}+e^{-B_kt}}{4}, \\ \lambda_1^k(t) = \lambda_2^k(t) &= \frac{1-e^{-B_kt}}{4}, \\ \lambda_3^k(t) &= \frac{1-2e^{-C_kt}+e^{-B_kt}}{4}, \\ \mu^k(t) &= (2S_k-1)\,\frac{1-e^{-B_kt}}{4}.\end{aligned} \tag{6}$$

For the $k$th qubit, the parameters $B_k$ and $C_k$ are, respectively, the decay rate of inversion and polarization, and $S_k \in [0,1]$ depends on the temperature of the bath. $S_k = 1$ corresponds to zero-temperature bath, and $S_k = 1/2$ the limit of infinite temperature [23]. Maps which are described by the above parameterization include, but are not restricted to, Pauli channels, dephasing, depolarizing, and amplitude damping [1,23].

The decohered state after time $t$ is obtained by the composition of the individual evolutions $\Lambda_k$, i.e., $\varrho(t) = \Lambda(|G_{(\mathcal{V},\mathcal{E})}\rangle\langle G_{(\mathcal{V},\mathcal{E})}|) := \Lambda_1\otimes\cdots\otimes\Lambda_N(|G_{(\mathcal{V},\mathcal{E})}\rangle\langle G_{(\mathcal{V},\mathcal{E})}|)$. The assumption of mutually independent environments is well justified whenever the separation between the vertices is large enough so that collective effects need not be taken into account.

To evaluate the computation fidelity after the noisy evolution, we note that once a measurement basis is defined, only the diagonal terms in such basis are relevant to the measurement outcome. The action of the channel (5) on a general measurement basis term $|M_{k_i}\rangle\langle M_{k_i'}|$ is such that nondiagonal ($k_i \neq k_i'$) terms are mapped onto nondiagonal terms, while diagonal ($k_i = k_i'$) terms evolve as

$$\begin{aligned}|M_{k_i}\rangle\langle M_{k_i}| \mapsto &(1-p_i)|M_{k_i}\rangle\langle M_{k_i}| + p_i|M_{k_i\oplus1}\rangle\langle M_{k_i\oplus1}| \\ &+ \text{off-diagonal terms},\end{aligned} \tag{7}$$

where henceforth we use a simplified notation whenever ambiguities are impossible.

In the equation above, $p_i$ is a function of time and of the parameters describing the channel (5). In the case of a measurement in the $x$-$y$ plane,

$$p_i^{xy} = \lambda_1^i(t) + \lambda_3^i(t), \tag{8}$$

and for a measurement in the $z$ direction it reads

$$p_i^z = 2\lambda_1^i(t) + (-1)^{k_i+1}2\mu^i(t). \tag{9}$$

As an example, consider the following two particular noise instances (which will be used later):

(i) Phase-flip error (pf) — With a probability $p_{\rm pf}/2$ the state $|0\rangle + |1\rangle$ is mapped onto $|0\rangle - |1\rangle$ and vice versa. This is obtained by setting $B_i = 0$ and $C_i = 2\Gamma_{\rm pf}$ in (5). Accordingly, the state evolution maps $\varrho_i \mapsto (1 - p_{\rm pf}/2)\varrho_i + p_{\rm pf}(Z\varrho_i Z)/2$, with $p_{\rm pf} = [1 - \exp(-2\Gamma_{\rm pf}\, t)]$. The impact of the decoherence on the measurement basis is then given by (8) and (9):

$$\begin{aligned} p_{i,{\rm pf}}^{xy} &= p_{\rm pf}/2, \\ p_{i,{\rm pf}}^{z} &= 0. \end{aligned} \tag{10}$$

(ii) White noise (w) — Add to the previous case the possibility of errors into the other independent directions $x$ and $y$. This causes the initial state to be exchanged with a maximally mixed one with probability $p_{\rm w}$. This is described by setting $S_i = 1/2$ and $B_i = C_i = 4\Gamma_{\rm w}$ in (5). Under this dynamics, the state evolves to $(1 - p_{\rm w})\varrho_i + p_{\rm w}\mathbb{1}/2$, with $p_{\rm w} = 1 - \exp(-4\Gamma_{\rm w}t)$. In this case we have

$$p_{i,{\rm w}}^{xy} = p_{i,{\rm w}}^{z} = p_{\rm w}/2. \tag{11}$$

It is important to notice that depending on the required measurement by an algorithm, some noisy maps might have no effect and the corresponding measurement outcomes are thus undisturbed. This feature will be further exploited in Sec. III A.

Note also that these decoherence processes can be interpreted as if the performed measurement was not perfect, being unable to distinguish between the two possible outcomes with probability $p_i$.

Now we are set to evaluate the fidelity of any one-way noisy quantum computation. Given a result $\vec{r}$ for the measurements, we want to determine $\mathcal{F}(|A_{\vec{r}}(\vec{\theta},\vec{\alpha})\rangle, \varrho_{\vec{r}})$, with $\varrho_{\vec{r}}$ the $(N - M)$ qubit state encoding the noisy protocol answer. We are thus interested in the projection of $\Lambda(|G_{(\mathcal{V},\mathcal{E})}\rangle\langle G_{(\mathcal{V},\mathcal{E})}|)$ onto $\bigotimes_{i=1}^{M} |M_{r_i}^{s_i(\vec{r})}\rangle\langle M_{r_i}^{s_i(\vec{r})}|$.

However, since $\langle M_{r_i}^{s_i(\vec{r})}|M_{k_i}^{s_i(\vec{k})}\rangle \neq 0$ in general, we first note that

$$\begin{aligned} \left|M_{k_i}^{s_i(\vec{k})}\right\rangle = \frac{1}{2}\Big\{&[1 + (-1)^{k_i} e^{-2i\theta_i[s_i(\vec{k})\oplus s_i(\vec{r})]}]\left|M_{0_i}^{s_i(\vec{r})}\right\rangle \\ &+ [1 - (-1)^{k_i} e^{-2i\theta_i[s_i(\vec{k})\oplus s_i(\vec{r})]}]\left|M_{1_i}^{s_i(\vec{r})}\right\rangle\Big\}, \end{aligned} \tag{12}$$

and therefore the state in (3) can be rewritten as

$$\begin{aligned} |G\rangle = \frac{1}{2^{\frac{3M}{2}}}\sum_{\vec{k}}\bigotimes_{i=1}^{M}\Big\{&[1 + (-1)^{k_i} e^{-2i\theta_i[s_i(\vec{k})\oplus s_i(\vec{r})]}]\left|M_{0_i}^{s_i(\vec{r})}\right\rangle \\ &+ [1 - (-1)^{k_i} e^{-2i\theta_i[s_i(\vec{k})\oplus s_i(\vec{r})]}]\left|M_{1_i}^{s_i(\vec{r})}\right\rangle\Big\}|A_{\vec{k}}\rangle. \end{aligned} \tag{13}$$

In the last two expressions above, when the measurement is in the $z$ direction there is no adaptation, i.e., $s_i = 0$.

Due to the noise, the components $|M_{0_i}^{s_i(\vec{r})}\rangle\langle M_{0_i}^{s_i(\vec{r})}|$ and $|M_{1_i}^{s_i(\vec{r})}\rangle\langle M_{1_i}^{s_i(\vec{r})}|$ mix according to the prescription in Eq. (7), reducing the fidelity of the protocol. The state after the action of the noise reads

$$\begin{aligned} \frac{1}{2^{3M}}\sum_{\vec{k},\vec{l}}\bigotimes_{i=1}^{M}\Big\{&[1 + (-1)^{k_i} e^{-2i\theta_i[s_i(\vec{k})\oplus s_i(\vec{r})]}][1 + (-1)^{l_i} e^{2i\theta_i[s_i(\vec{l})\oplus s_i(\vec{r})]}]\Big[(1 - p_i)\left|M_{0_i}^{s_i(\vec{r})}\right\rangle\!\left\langle M_{0_i}^{s_i(\vec{r})}\right| + p_i\left|M_{1_i}^{s_i(\vec{r})}\right\rangle\!\left\langle M_{1_i}^{s_i(\vec{r})}\right|\Big] \\ &+ [1 - (-1)^{k_i} e^{-2i\theta_i[s_i(\vec{k})\oplus s_i(\vec{r})]}][1 - (-1)^{l_i} e^{2i\theta_i[s_i(\vec{l})\oplus s_i(\vec{r})]}]\Big[(1 - p_i)\left|M_{1_i}^{s_i(\vec{r})}\right\rangle\!\left\langle M_{1_i}^{s_i(\vec{r})}\right| + p_i\left|M_{0_i}^{s_i(\vec{r})}\right\rangle\!\left\langle M_{0_i}^{s_i(\vec{r})}\right|\Big] \\ &+ \text{ of-diagonal terms}\Big\}\Lambda(|A_{\vec{k}}\rangle\langle A_{\vec{l}}|). \end{aligned} \tag{14}$$

The projection onto the subspace corresponding to $\vec{r}$ leads the remaining $N - M$ qubits in the state

$$\begin{aligned} \varrho_{\vec{r}} = \frac{1}{2^{3M}}\frac{1}{\mathcal{Z}_{\vec{r}}}\sum_{\vec{k},\vec{l}}\prod_{i}^{M}\{&(1 - p_i)[1 + (-1)^{k_i+r_i} e^{-2i\theta_i[s_i(\vec{k})\oplus s_i(\vec{r})]}][1 + (-1)^{l_i+r_i} e^{2i\theta_i[s_i(\vec{l})\oplus s_i(\vec{r})]}] \\ &+ p_i[1 - (-1)^{k_i+r_i} e^{-2i\theta_i[s_i(\vec{k})\oplus s_i(\vec{r})]}][1 - (-1)^{l_i+r_i} e^{2i\theta_i[s_i(\vec{l})\oplus s_i(\vec{r})]}]\}\Lambda(|A_{\vec{k}}\rangle\langle A_{\vec{l}}|), \end{aligned} \tag{15}$$

with $\mathcal{Z}_{\vec{r}}$ the probability of obtaining the outcome $\vec{r}$. Note that in the above expression, the channels acting in each qubit can be different and might influence the state for different time intervals. This is an important feature for the qubits might be of a different nature and could be measured at different times.

We are thus in a position to evaluate the computation fidelity $\mathcal{F}_{\rm OneWay}(\vec{r}) = \langle A_{\vec{r}}|\varrho_{\vec{r}}|A_{\vec{r}}\rangle$ for the decohered graph state, to get

$$\begin{aligned} \mathcal{F}_{\rm OneWay}(\vec{r}) = \frac{1}{2^{3M}}\frac{1}{\mathcal{Z}_{\vec{r}}}\sum_{\vec{k},\vec{l}}\prod_{i}^{M}\{&(1 - p_i)[1 + (-1)^{k_i+r_i} e^{-2i\theta_i[s_i(\vec{k})\oplus s_i(\vec{r})]}][1 + (-1)^{l_i+r_i} e^{2i\theta_i[s_i(\vec{l})\oplus s_i(\vec{r})]}] \\ &+ p_i[1 - (-1)^{k_i+r_i} e^{-2i\theta_i[s_i(\vec{k})\oplus s_i(\vec{r})]}][1 - (-1)^{l_i+r_i} e^{2ii[s_i(\vec{l})\oplus s_i(\vec{r})]}]\}A_{\vec{r},\vec{k},\vec{l}} \end{aligned} \tag{16}$$

with $A_{\vec{r},\vec{k},\vec{l}} = \langle A_{\vec{r}}|\Lambda(|A_{\vec{k}}\rangle\langle A_{\vec{l}}|)|A_{\vec{r}}\rangle$.

Instead of looking for the fidelity of a particular outcome $\vec{r}$ of the computation, one is often more interested in the average fidelity over all the outcomes, simply given by

$$\overline{\mathcal{F}}_{\rm OneWay} = \sum_{\vec{r}} \mathcal{Z}_{\vec{r}}\mathcal{F}_{\rm OneWay}(\vec{r}). \tag{17}$$

With this expression in hand and the results in [24], which allow for the evaluation of noisy graph-state entanglement, one can compare the dynamics of entanglement in the state used as a resource with the fidelity dynamics of *any* noisy one-way computation. Furthermore, from the expression (16) one can immediately infer that the computation fidelity shows a continuous decay in time, as each $p_j$ is a continuous function of time. That is in clear contrast with a generic entanglement evolution, where the amount of entanglement may vanish in finite time [25]. As noted in [17] (considering the particular effects of individual decoherence in a four-qubit cluster state), the finite time disentanglement does not cause changes in the behavior of the computation fidelity. Entanglement decay is shown here, in great generality, to not display a one-to-one correlation with computation quality.

### A. Computations without adaptations

Computations that need no adaptations (NA) turn out to be a very interesting subset of all possible computations. If a computation requires no adaptations, $s_i(\vec{k}) = 0\ \forall i$ and $\forall \vec{k}$, then all the outcomes happen with the same probability, $\mathcal{Z}_{\vec{r}} = 1/2^M\ \forall \vec{r}$. In this case, Eq. (16) simplifies to

$$\mathcal{F}^{\mathrm{NA}}_{\mathrm{OneWay}}(\vec{r}) = \sum_{\vec{k}} \prod_{i}^{M} (1-p_i)^{1\oplus k_i \oplus r_i}\, p_i^{k_i \oplus r_i}\, A_{\vec{r},\vec{k},\vec{k}}\ . \quad (18)$$

Expression (18) shows that the overall effect of quite general decoherence processes, as parametrized in (5), over the nonadaptive measured qubits is to incoherently combine all the possible noisy answers associated with such measurements. The sign Boolean function $f_{\mathrm{Sig}}$ in the definition of the by-products (4) can, also in such cases, be safely ignored.

Further simplification is possible for nonadaptive computations when the channel acting on the answer qubits is given by a Pauli map $\Gamma$, obtained by setting $\mu(t) = 0$ in the general expression (5). In this case $\Gamma[B_{\vec{k}}|A_{\vec{0}}\rangle\langle A_{\vec{0}}|B^{\dagger}_{\vec{k}}] = B_{\vec{k}}\Gamma[|A_{\vec{0}}\rangle\langle A_{\vec{0}}|]B^{\dagger}_{\vec{k}}$ and $A_{\vec{r},\vec{k},\vec{k}} = A_{\vec{0},\vec{r}\oplus\vec{k},\vec{r}\oplus\vec{k}}$, which implies that $\mathcal{F}^{\mathrm{NA}}_{\mathrm{OneWay}}(\vec{r}) = \mathcal{F}^{\mathrm{NA}}_{\mathrm{OneWay}}(\vec{0})$. The average fidelity (17) is then the same as the fidelity of any outcome, tremendously simplifying its evaluation.

A greater insight on the nature of correlations necessary for a one-way computation without adaptations is possible when considering noise of the form

$$\Lambda_j(\bullet) = (1-p_j)\bullet + p_j R_{\hat{n}_j}(\phi_j)\bullet R^{\dagger}_{\hat{n}_j}(\phi_j), \quad (19)$$

with $R_{\hat{n}_j}(\phi_j) = \exp(-i\phi_j \hat{n}_j \cdot \vec{\sigma}/2)$ a rotation around the axis $\hat{n}_j$ in the Bloch sphere. This map has two invariant states, the eigenvectors $|\hat{n}_{j\,0,1}(\phi_j)\rangle$ of the rotation. Now remember that a measurement in a certain basis can be done directly on it, or by first applying a unitary transformation to a convenient basis and then the measurement. It stands for a simple relabelling. Therefore for all nonadaptive measurements (NAMs), if the noise is of the type in (19), it is possible to find $U(\phi_j,\theta_j,\alpha_j)$ that transforms $|M_{k_j}(\theta_j,\alpha_j)\rangle \to |\hat{n}_{j\,k_j}(\phi_j)\rangle$. This perfectly protects the outcome probability distribution of the NAMs, even for highly mixed resource states, as the measurement outcomes will not be affected. For computations in which all the $N$ qubits are measured in a nonadaptive fashion, this procedure protects the whole computation, and the graph state can be exchanged by a mixed state which bears only classical correlations — that is, a separable mixed state that can be written in a basis formed by the tensor product of single-qubit orthonormal basis [26]. The noisy computation without adaptations can thus be classically simulated.

To exemplify this, consider the state in which the $i$th qubit is to be measured in the $X$ basis, namely,

$$|G_N\rangle = \frac{1}{\sqrt{2}}(|+_i\rangle|A_+\rangle + |-_i\rangle|A_-\rangle), \quad (20)$$

with $|A_\pm\rangle = (1/\sqrt{2})(|G_{N-1}\rangle \pm \bigotimes_{j\in\mathcal{N}_i} Z_j|G_{N-1}\rangle)$, and $\mathcal{N}_i$ the neighbors of the $i$th qubit. Applying a bit-flip channel $\Lambda^X_i(\bullet) := (1-p)\bullet + pX\bullet X$ on the $i$th qubit decreases the entanglement between this qubit and the rest of the graph, while it does not affect the measurement outcome. Therefore, since applying $X$ on a qubit $i$ of a graph is equivalent to apply $Z$'s in all its neighbors $\mathcal{N}_i$ [23], preparing the state

$$\frac{1}{2}\left(|G_N\rangle\langle G_N| + \prod_{j\in\mathcal{N}_i} Z_j |G_N\rangle\langle G_N| \prod_{j\in\mathcal{N}_i} Z_j\right) = \frac{1}{2}(|+_i\rangle\langle +_i| \otimes |A_+\rangle\langle A_+| + |-_i\rangle\langle -_i| \otimes |A_-\rangle\langle A_-|), \quad (21)$$

which is a separable state between the $i$th qubit and the rest of the graph state and is invariant under the application of bit flip to the $i$th qubit, leads to the same probability distribution of outcomes for a measurement of the $i$th qubit on the $X$ basis. Moreover, it generates the same answers $\{|A_\pm\rangle\}$, and this procedure can be iterated to the remaining qubits to be measured nonadaptively.

The NAMs are related to the so-called Clifford-group transformations of part of a quantum protocol, and as such can be simulated efficiently in a classical computer [4,10,27]. From the framework presented here, it is clear that the entanglement between the qubits to be measured nonadaptively and the rest of the graph state can be interchanged by simple classical correlations encoded in a mixed-state without compromising the computation. When adaptations are necessary this scheme cannot prevail. Adaptive measurements are thus related to the quantum part of the computation, where some resilient entanglement may be of use.

## IV. APPLICATIONS

In the following we apply the formulas developed above to specific examples and compare the fidelity dynamics of noisy one-way quantum computations to the entanglement decay of the resource state. In general, a mismatch between the two dynamics is found: higher entanglement is not connected with higher quality computations.

### A. Remote state preparation (RSP)

Take the simplest possible one-way protocol, i.e., to remotely prepare the single-qubit state $\cos(\phi/2)|0\rangle - i\sin(\phi/2)|1\rangle$ [15]. Within the one-way model, we start with a graph state of two qubits, $|G_2\rangle = (|00\rangle + |01\rangle + |10\rangle - |11\rangle)/2$, and apply a measurement on the first qubit to produce

the desired state on the second one. For this task, one chooses to measure the observable with eigenvectors $|M_k(\phi,\pi/2)\rangle = [|0\rangle + (-1)^k \exp(-i\phi)|1\rangle]/\sqrt{2}$, where $k \in \{0,1\}$ represents the two possible measurement outcomes. After the measurement, the second qubit is left in the state $|\Psi_{\rm out}\rangle = X^k[\cos(\phi/2)|0\rangle - i\sin(\phi/2)|1\rangle]/\sqrt{2}$. Apart from the by-product $B_k = X^k$, which is known, the desired state is obtained with maximal fidelity. However, quantum computations are prone to errors. Let us assume, for simplicity, a favorable scenario where only the first qubit (the one to be measured) is subjected to noise. The initial two-qubit state evolves then to $(\Lambda_1 \otimes \mathbb{1})(|G_2\rangle\langle G_2|)$. Since no adaptations are necessary and the second qubit is not under the action of an environment, the mean fidelity for this protocol, as evaluated by (18), reads

$$\overline{\mathcal{F}}_{\rm RSP} = \mathcal{F}_{\rm RSP}(0) = (1-p_1)A_{0,0,0} + p_1 A_{0,1,1}. \tag{22}$$

If the measurement is on the $x$-$y$ plane, then $p_1 = p_1^{xy}$. Furthermore, $A_{0,0,0} = |\langle A_0|A_0\rangle|^2 = 1$ and $A_{0,1,1} = |\langle A_0|X|A_0\rangle|^2 = 0$. This leads to $\mathcal{F}_{\rm RSP} = (1-p_1^{xy})$, which now depends only on the specific nature of the noise acting on the first qubit.

To address the connection between computation fidelity and entanglement, consider the two instances of open system dynamics introduced in Sec. III:

(i) Phase-flip error (pf) — The state evolution maps $|G_2\rangle\langle G_2| \mapsto (1-p_{\rm pf}/2)|G_2\rangle\langle G_2| + p_{\rm pf}/2(Z\otimes\mathbb{1})|G_2\rangle\langle G_2|(Z\otimes\mathbb{1})$, with $p_{\rm pf} = [1-\exp(-2\Gamma_{\rm pf}\,t)]$. The entanglement dynamics of the noisy resource state can be inferred by its concurrence [28], $C^{\rm pf}_{\rm RSP}(t) = \exp(-2\Gamma_{\rm pf}t)$. Now, applying the state preparation protocol described above to the decohered state, the output fidelity, given that $p_1^{xy} = p_{\rm pf}/2$, is $\mathcal{F}^{\rm pf}_{\rm RSP}(t) = [1+\exp(-2\Gamma_{\rm pf}\,t)]/2$. The correlation between decreasing entanglement with decreasing fidelity is as supposed.

(ii) White noise (w) — By adding noise to the other independent directions, the resource state evolves to $(1-p_{\rm w})|G_2\rangle\langle G_2| + p_{\rm w}\mathbb{1}/4$, with $p_{\rm w} = 1-\exp(-4\Gamma_{\rm w}t)$. As before, we evaluate the entanglement dynamics via concurrence, $C^{\rm w}_{\rm RSP}(t) = \max\{0,[3\exp(-4\Gamma_{\rm w}t)-1]/2\}$. Finally, the protocol fidelity with white noise, $p_1^{xy} = p_{\rm w}/2$, reads $\mathcal{F}^{\rm w}_{\rm RSP}(t) = [1+\exp(-4\Gamma_{\rm w}t)]/2$. Once again, a smaller value of entanglement leads to a worse computation.

Nevertheless, a comparison between both situations shows unexpected behavior (see Fig. 1): the computation fidelity is higher when the entanglement is more fragile against disturbances. Note that even after the entanglement is fully exhausted, the white noise case still outperforms the always entangled phase-flip case. Even in the simplest one-way protocol the entanglement is neither *sufficient* nor a *necessary* signature of higher quality for the noisy quantum computation.

In fact, this reasoning can be extended to quantum discord, a recently proposed measure of quantum correlations which does not include only entanglement [31]. This measure attracted lots of attention lately, since it seems to pinpoint efficient quantum computations even in the apparent absence of entanglement [6]. Quantum discord is defined as $\mathcal{Q}(\varrho) = \mathcal{I}(\varrho) - \mathcal{C}(\varrho)$, where the mutual quantum information

$$\mathcal{I}(\varrho) = S(\varrho_A) + S(\varrho_B) - S(\varrho) \tag{23}$$

is a measure of total correlations, and

$$\mathcal{C}(\varrho) = \sup_{\{\Pi_k\}} S(\varrho_A) - S\big(\varrho_A^k|\{\Pi_B^k\}\big) \tag{24}$$

is a measure of classical correlations, with the supremum taken over all sets of orthogonal projectors $\{\Pi_B^k\}$. As usual, $S(\varrho) = -{\rm Tr}(\varrho\log_2\varrho)$ denotes the von Neumann entropy, and $\varrho_i = {\rm Tr}_{j\neq i}(\varrho)$ with $i,j = A,B$ is the partial density matrix. For classical systems $\mathcal{I} = \mathcal{C}$, and thus equivalent definitions for the mutual information, resulting in zero quantum discord.

Evaluating the quantum discord, as shown in Ref. [32], for the toy protocol described above shows that a lower quantum discord may lead to a higher computation fidelity (see Fig. 2). Also quantum discord cannot be employed to signal higher quality in a noisy quantum computation scenario.

As a last possible signature of a higher quality noisy quantum computation, we may employ the measure of nonclassicality very recently proposed in [33] (see also [34] for a slightly different but equivalent approach), namely, the minimum entanglement potential ($\mathcal{P}_{\rm ME}$) of a given state $\varrho_A$. As a result of the following activation protocol (see [33] for details),

(i) Act with local unitaries $U_A$ in each subsystem of $\varrho_A$,

(ii) Interact, through a controlled-NOT (CNOT), each subsystem of $\varrho_A$ with an ancilla initialized in the state $|0\rangle$,

any nonclassical state becomes entangled (for any choice of $U_A$) with the ancillary system A'. The minimum entanglement generated across the $A:A'$ split quantifies the nonclassicality of state, that is,

$$\mathcal{P}_{\rm ME}(\varrho_A) = \min_{U_A} E_{A:A'}(\varrho'_{A:A'}), \tag{25}$$

where $\varrho'_{A:A'}$ is the system-ancilla state generated in the end of the activation protocol.

Choosing as a measure of entanglement the negativity [29], we can readily compute the $\mathcal{P}_{\rm ME}$ for the resource state in the two noise scenarios mentioned above. In these cases we get $M(\Lambda^{\rm pf/w}[|G_2\rangle\langle G_2|]) = (1-p^{\rm pf/w}) =: (\mathcal{P}_{\rm ME})^{\rm pf/w}_{\rm RSP}$. For the RSP protocol the relation $(\mathcal{P}_{\rm ME})^{\rm pf/w}_{\rm RSP} = 2\mathcal{F}^{\rm pf/w}_{\rm RSP} - 1$ then holds, and therefore a higher $\mathcal{P}_{\rm ME}$ implies higher computation quality. At least for this simple example, the nonclassicality of the

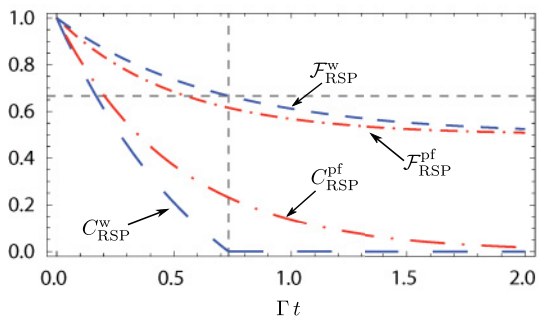


FIG. 1. (Color online) RSP: Entanglement decay vs computation fidelity ($\Gamma_{\rm w} = 0.375\,\Gamma_{\rm pf} = \Gamma$). A less entangled state may lead to a higher computation fidelity (the same ordering is obtained if the negativity [29] is used instead of concurrence). In the white noise case, entanglement vanishes when the fidelity reaches 2/3 (horizontal dashed line) [30]. Entanglement is thus superfluous for achieving fidelities below this threshold.

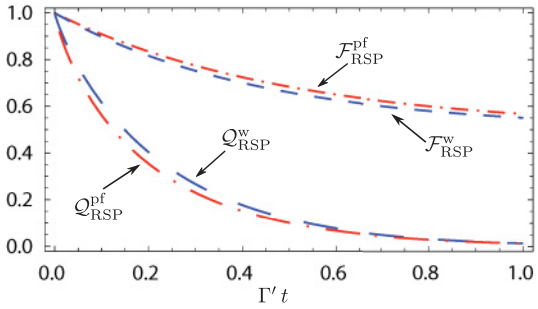


FIG. 2. (Color online) RSP: Quantum discord decay vs computation fidelity ($\Gamma_w = 0.57\,\Gamma_{pf} = \Gamma'$). As for concurrence, a state with less quantum discord may lead to a better-quality computation. Quantum discord vanishes only asymptotically.

resource state, quantified by the minimum entanglement potential, seems to be correlated to the quality of the computation.

### B. Primitives for universal quantum computation

The basic gates for universal quantum computation are a generic single-qubit rotation ($R$) and a two-qubit controlled operation, say, a controlled-not (CNOT) gate. How is the fidelity of these basic building blocks related to the entanglement of their resource states?

Any U(2) rotation can be decomposed into successive rotations over three different angles, known as the Euler angles, as $R(\phi_1,\phi_2,\phi_3) = R_{\hat{x}}(\phi_3)R_{\hat{z}}(\phi_2)R_{\hat{x}}(\phi_1)$. Any qubit state can be created out of any other qubit state via this operation. Within the one-way framework this task is implemented via adaptive measurements in a five-qubit cluster state [10]. The measurement pattern and required adaptations are depicted in Fig. 3(a). Given that the input qubit was initially in the state

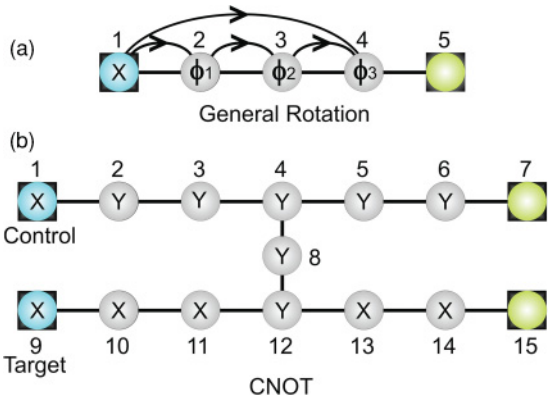


FIG. 3. (Color online) Universal gates: One-way implementation of a universal set of gates. The blue qubits encode the initial state, and the green ones the output state after the measurements. Gray qubits represent intermediate steps of the computation. All the measurements required are in the $xy$ plane ($\alpha_i = \pi/2$), with the latitude angle $\theta_i$ specified for each qubit in the picture. (a) Single-qubit rotation. A general rotation requires adaptive measurements, which are indicated by the arrows above. These arrows are translated into the adaptation parameter for each qubit as $s_1(\vec{k}) = 0, s_2(\vec{k}) = k_1, s_3(\vec{k}) = k_2$, and $s_4(\vec{k}) = k_1 + k_3$. (b) Controlled-NOT. Despite that this is an entangling gate, it requires no adaptations. This means that once the input state is defined, it can be classically simulated (see Sec. III A).

$|\psi_{in}\rangle$, after a execution of this protocol with outcomes $\vec{r}$, the output qubit is left on $B_{\vec{r}}\,R(\phi_1,\phi_2,\phi_3)|\psi_{in}\rangle$. The by-products $B_{\vec{k}}$ of this computation are defined as in (4) with

$$f_{5,Sig}(\vec{k}) = k_3k_2;$$
$$f_{5,X}(\vec{k}) = k_4 + k_2;$$
$$f_{5,Z}(\vec{k}) = k_3 + k_1.$$

For the CNOT gate a cluster of 15 qubits is necessary, but no adaptations are required [10]. The measurement pattern defining the algorithm is shown in Fig. 3(b). The CNOT acts on two qubits, called target and control, such that if the control is in the state $|1\rangle\langle 1|$ the target qubit is flipped and nothing happens otherwise, that is, $\text{CNOT}_{ij} = |0_i\rangle\langle 0_i| \otimes \mathbb{1}_j + |1_i\rangle\langle 1_i| \otimes X_j$. If the initial control-target state in the qubits 1 and 9 is $|\chi_{in}\rangle$, the outcome state in the qubits 7 and 15, after measurements with outcome $\vec{r}$, is $|\chi_{out}\rangle = B_{\vec{r}}\ \text{CNOT}|\chi_{in}\rangle$. The by-products of this operation are given by setting

$$f_{7,X}(\vec{k}) = k_2 + k_3 + k_5 + k_6;$$
$$f_{15,X}(\vec{k}) = k_2 + k_3 + k_8 + k_{10} + k_{12} + k_{14};$$
$$f_{7,Z}(\vec{k}) = k_1 + k_3 + k_4 + k_5 + k_8 + k_9 + k_{11} + 1;$$
$$f_{15,Z}(\vec{k}) = k_9 + k_{11} + k_{13}.$$

As no adaptations are necessary for this gate, we can ignore the Boolean function $f_{Sig}$.

Now consider that all measured qubits, for both protocols, are under the influence of identical local environments ($p_i = p$). As before we consider the cases of phase-flip and white noise. The noisy evolution of the fidelity for the rotation protocol, $\mathcal{F}_R^{w/pf}$, can be assessed by expressions (16) and (17). For the CNOT gate, however, the dynamics of $\mathcal{F}_{CNOT}^{w/pf}$ is obtained via Eq. (18), with no need of averaging over the possible measurement outcomes. For both protocols do not need measurements along the $z$ direction, if we have $p^w_{xy} = p^{pf}_{xy}$, then the fidelity decay under the two kinds of

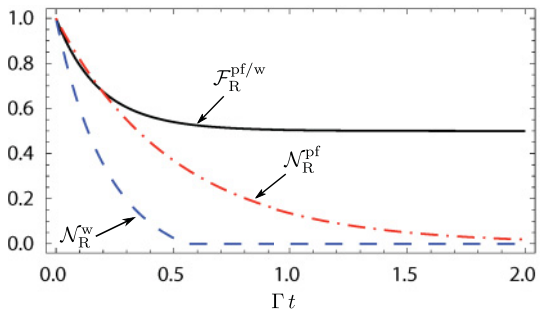


FIG. 4. (Color online) $R$: Entanglement decay vs computation quality. Noisy rotation of the initial state $|\psi_{in}\rangle = |0\rangle$ setting $\phi_1 = \phi_2 = \phi_3 = \pi/4$, when $p_w = p_{pf}$, i.e., $\Gamma_{pf} = 2\Gamma_w = \Gamma$. In this case, $\mathcal{F}_R^{pf} = \mathcal{F}_R^{w}$, represented by the solid black line. Nevertheless, the entanglement dynamics differs for each noisy instance. The entanglement between the output qubit with the remaining of the cluster, as estimated by the negativity [29], is depicted by the dashed blue line for the white noisy case ($\mathcal{N}_R^w$), and by the dot-dashed red line for phase flip ($\mathcal{N}_R^{pf}$). A lower amount of entanglement can thus yield as good a computation as a higher amount. A similar result holds for the CNOT gate.

noise is exactly the same. That is, for both noisy scenarios $\mathcal{F}_R^{\rm pf} = \mathcal{F}_R^{\rm w}$ and $\mathcal{F}_{\rm CNOT}^{\rm pf} = \mathcal{F}_{\rm CNOT}^{\rm w}$. This is in stark contrast to the entanglement decay of the resource states which will be generically different under the two noise instances. See Fig. 4 for a quantitative account of this fact. This once more shows that entanglement dynamics is detached from the fidelity dynamics, and as such a less entangled state can lead to higher (or equal) quality computations.

### C. Deutsch-Jozsa (DJ) algorithm

Let $f : \{0,1\}^N \mapsto \{0,1\}$ be an unknown Boolean function which can be either constant, with all entries giving the same answer, or balanced, with half of the entries yielding 0 and the other half 1. What is the minimum number of times one has to query an Oracle that implements $f$ to discover the function's type? Classically, in general, one needs at least $2^{N-1}+1$ queries. Quantum mechanically, a single query via the DJ algorithm is sufficient [12]. In the quantum version, the Oracle applies a unitary $U_f$ on the $N$ qubits of the input state plus an auxiliary qubit ($A$) as follows: $U_f|x\rangle|y\rangle = |x\rangle|y \oplus f(x)\rangle$, where $x$ and $y$ are the decimal representations of binary strings. The DJ algorithm takes advantage of the superposition principle to evaluate all the entries at once and can be cast as the unitary $D = H^{\otimes(N+1)}\, U_f\, H^{\otimes(N+1)}$, with $H = 1/\sqrt{2}(|0\rangle\langle 0| + |0\rangle\langle 1| + |1\rangle\langle 0| - |1\rangle\langle 1|)$ the Hadamard gate. It is a simple calculation to deduce that $D(|0\rangle^{\otimes N}|1\rangle)$ leads to the outcome $\vec{0}$, after measurement of the $N$ qubits in the computational basis, if and only if $f$ is constant. This is clearly spelled out by the state below:

$$D(|0\rangle^{\otimes N}|1\rangle) = H^{\otimes N+1}\frac{1}{2^{N/2}}\sum_{i=0}^{2^N-1}(-1)^{f(i)}|i\rangle|-\rangle. \qquad (26)$$

If $f$ is constant the final state gets only a global phase $(-1)^{f(0)}$ in relation to the initial state (remember that $H^2 = \mathbb{1}$). In its noiseless implementation, the DJ is known to generically create entanglement [13]. Note that along all the protocol the auxiliary qubit is never entangled with the $N$-qubit principal system. However, depending on the function $f$ that the Oracle implements, the $N$-qubit system can become entangled. For a constant function $f$ the state is never entangled, as can be readily seen from (26). Despite that, for example, the balanced function $f : \{0,1\}^3 \to \{0,1\}$ with truth table,

| $x$ | $f(x)$ |
|---|---|
| $0 = 000$ | 0 |
| $1 = 001$ | 0 |
| $2 = 010$ | 0 |
| $3 = 011$ | 1 |
| $4 = 100$ | 1 |
| $5 = 101$ | 1 |
| $6 = 110$ | 1 |
| $7 = 111$ | 0 |

generates an entangled state during the execution of the DJ protocol [35]. For three qubits this balanced function can be performed by the unitary operation $U_f = \text{CNOT}_{1,A}\text{CZ}_{2,3}$,

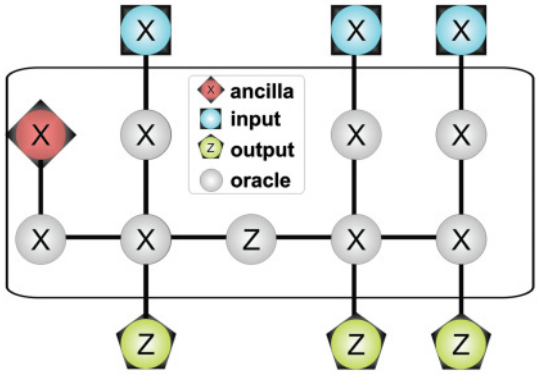


FIG. 5. (Color online) Graph-state and measurement pattern for the DJ protocol simulating the balanced function $U_f = \prod_{i=2}^{N-1} Z_{i,i+1}^{(C)}\text{CNOT}_{1,A}$. All the qubits are measured without adaptations, and so the entangled graph state can be replaced by a mixed state with only classical correlations (see Sec. III A).

and can be easily generalized for $N$ qubits as $U_f = \text{CNOT}_{1,A}\bigotimes_{i=2}^{N-1}\text{CZ}_{i,i+1}$. Note that the operation $U_f$ can be done within the one-way framework by measurements without any adaptations (see Fig. 5).

On the other hand, a noisy implementation of the DJ, still within the circuit model, was analyzed in [36] and shown to present a small but finite advantage over its classical counterpart, even for fully separable states. This indicates that to unveil the role of the entanglement in the mixed DJ protocol one has to split the generation and use of entanglement. In the one-way setting the DJ problem can be posed as follows [37]: the Oracle prepares a graph state that allows her to implement a function $f$ by local measurements. She hands to Neo (the user) a set of input qubits and a set of output qubits. By encoding (through measurements) a certain value $x$ into the input qubits, Neo can read out $f(x)$ in the output qubits. As before, an appropriate choice of measurements allows Neo to discover whether the function is constant or balanced in a single run of the protocol.

In the example shown in Fig. 5, neither the implementation of $f$ nor the measurements by Neo require adaptations. It is thus possible for the Oracle to interchange the NAMs in a entangled graph state with a mixed state without any entanglement, and even though Neo can decide whether $f$ is constant or balanced in a single query. To design such a classically correlated state the Oracle proceeds as follows: (i) Think of the original cluster state needed to encode the desired function for any input. (ii) Apply to it a hypothetical noise of the type in (19), but protecting the measurement outcomes by rotating the qubits to a convenient basis. In this step the Oracle can only protect a single instance of input states, and she does that for the $H^{\otimes N}|\vec{0}\rangle$. (iii) Finally, she evaluates the stationary state of the decoherence process and rotates the qubits back to their original basis. The resulting (theoretical) state can be effectively prepared by the Oracle only by classical means, and it is ready to be handed in to Neo. If now Neo performs the correct set of measurements on the input qubits, the output qubits will encode whether the function is constant or balanced. It is interesting to notice that despite the fact the state bears only classical correlations, the quantum

possibility of measuring on a different basis entails advantages over a fully classical implementation. In fact, many Boolean functions, that in a circuit model generate entangled states, can be decomposed into combinations of CZs, CNOTs, $H$'s, and possible relabelling of the qubits, transformations that can be attained within the one-way model without adaptations. As such, they can be simulated by a classically correlated resource state. These ideas, therefore, extend to many algorithms, for instance, to the Simon's [38] algorithm, as long as the function evaluated by the Oracle does not require adaptations. An interesting question, that we leave open, is to determine the fraction of Boolean functions that can be evaluated without adaptations.

### D. Ancilla-driven quantum computation

The idea used in Sec. III can be readily applied to the ancilla-driven model of quantum computation [14]. In this model all the necessary unitary transformations to be realized in a quantum register are done through measurements in an ancillary qubit coupled to the register. A coupling interaction given simply by $E = H_a\, H_{r_i}\, \mathrm{CZ}_{ar_i}$ is sufficient to allow for universal quantum computation. The index $a$ represents the ancilla and $r_i$ the $i$th qubit of the quantum register. After the interaction the ancilla is measured in the same basis (2) of the usual one-way model (see Fig. 6 for details).

The effects of an inaccurate measurement (the projection direction is deviated from the ideal one) in the fidelity of the ancilla-driven quantum computation was analyzed in [20]. There it was shown that for a faulty measurement, the more the qubit being coupled to the ancilla is entangled with the rest of the qubits in the register, the smaller the mean fidelity of the operation. The relation is given by

$$\overline{\mathcal{F}} \leqslant 1 - S_L \sin^2 \frac{\epsilon}{2}, \tag{27}$$

where the entanglement is quantified by $S_L = 2[1 - \mathrm{Tr}(\varrho_{r_i}^2)]$, the normalized linear entropy of the reduced density matrix $\varrho_{r_i}$, and $\epsilon$ quantifies the angular deviation from the ideal measurement. Here we derive an analogous expression, but instead of an inaccurate measurement we consider that the ancilla qubit is undergoing one of the decoherence processes described by the map (5). In this scenario we arrive at the relation

$$\overline{\mathcal{F}} \leqslant 1 - p\, S_L, \tag{28}$$

which is fully equivalent to (27). For a given amount $S_L$ of entanglement we can thus estimate how small the decoherence parameter $p$ should be, such that the computation fidelity is not below a given threshold.

The derivation of (28) follows the same ideas as in Ref. [19]. Consider that the register state $|\psi_r\rangle$ is given by

$$|\psi_r\rangle = \alpha|0\rangle|\eta_0\rangle + \beta|1\rangle|\eta_1\rangle. \tag{29}$$

After the interaction of a register-qubit with the ancilla (initialized in $|+\rangle$), the register-ancilla state $|\phi_{ar}\rangle$ is given by (see Fig. 6(a))

$$|\phi_{ar}\rangle = \alpha|0\rangle_a|+\rangle|\eta_0\rangle + \beta|1\rangle_a|-\rangle|\eta_1\rangle \tag{30}$$

$$= \frac{1}{\sqrt{2}}(|M_0\rangle_a|A_0\rangle + |M_1\rangle_a|A_1\rangle), \tag{31}$$

where $|A_k\rangle = \alpha|+\rangle|\eta_0\rangle + (-1)^k e^{i\phi}\beta|-\rangle|\eta_1\rangle$. From the results of the Sec. III we know that the effect of a map (5) on the ancilla is to mix the answers of the computation. It is straightforward to calculate the mean fidelity $\overline{\mathcal{F}} = \mathcal{Z}_0\mathcal{F}(0) + \mathcal{Z}_1\mathcal{F}(1)$ (with $\mathcal{Z}_k$ the probability of measuring $|M_k\rangle$ with a associated fidelity $\mathcal{F}_k$) given by

$$\overline{\mathcal{F}} = 1 - p(1 - \xi^2), \tag{32}$$

where $\xi = \mathrm{Tr}(Z_k\varrho_k)$. Since $S_L \leqslant 1 - [\mathrm{Tr}(Z_i\varrho_i)]^2$ we immediately obtain relation (28). The same result holds for the situation where the ancilla is coupled to two qubits of the register state (see Fig. 6(b)).

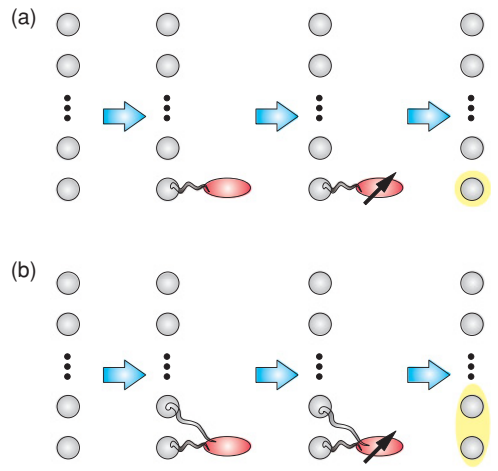


FIG. 6. (Color online) (a) Single-qubit rotation. After the interaction $E = H_a\, H_{r_i}\, \mathrm{CZ}_{ar_i}$ between the $i$th qubit on the register and the ancilla, the latter is measured in the $(|0\rangle \pm e^{i\phi}|1\rangle)/\sqrt{2}$ basis. As a result the transformation $X^k H R_{\hat{z}}(\phi)$ is applied to the qubit in the register (with $k$ the classical outcome of the measurement). (b) Two-qubit entangling gate. After the interaction the ancilla is measured in the basis $\{|0\rangle, |1\rangle\}$, and as a result the two qubits on the register undergo the transformation $(X_i^k H_i \otimes H_j)\mathrm{CZ}_{ij}$.

## V. CONCLUSION

In this paper we have shown that the effect of very general local decoherence maps on the measurement bases employed by the one-way model is to mix the two measurement directions with a certain weight $p$, which characterizes the map. With this observation the fidelity of any computation within the one-way model can be readily obtained. This allowed us to conclude that the impact of the noise on the entanglement in the resource state is not generically related to loss of computation quality.

Even for the simplest one-way protocol, the remote-state preparation (Sec. IV A), a state with more entanglement (or discord) does not necessarily yield a higher quality computation. In other words, robust entanglement does not mean robust one-way quantum computations. Rather on the contrary, for the ancilla-driven measurement-based computation model

(Sec. IV D), the fidelity sensitivity to decoherence is bigger the higher the entanglement in the resource state.

Even more surprisingly, the framework developed here made clear that the parts of algorithms that do not require adaptations can be replaced by a classically correlated resource state. This implies, for example, that some instances of the Deutsch-Josza algorithm can be realized in the one-way paradigm without any entanglement (Sec. IV C).

Thus, if entanglement (discord) cannot be assigned as the signature of efficient noisy quantum computations, which other quantities may assume this role? For the RSP protocol, the amount of nonclassicality in the resource state (quantified by the minimum entanglement potential) seems to also point out the computation quality (Sec. IV A). We believe that it would be interesting to extend or falsify this connection between nonclassicality and computation fidelity to more general cases.

All these results show that entanglement may not be the most important resource for the quality of noisy quantum computations. The mere use of a quantum logic, in a mixed-state scenario, seems to entail considerable gain over classical computations. This has obvious implications to experimental implementation of quantum information processes, for it relaxes the required isolation of the quantum system from its environment. In fact, this can shed some light on the functioning of biological systems, which, despite being strongly influenced by the surroundings, are mesoscopic systems that may profit from their quantum nature [39].

## ACKNOWLEDGMENTS

We would like to acknowledge Tomoyuki Morimae for comments and for pointing out Refs. [19,20]. R.C. was funded by PROBRAL CAPES/DAAD, Faperj, and the Q-Essence projects. F.M. was supported by the Alexander von Humboldt Foundation and the Belgian Interuniversity Attraction Poles Programme P6/02.

[1] M. A. Nielsen and I. L. Chuang, *Quantum Computation and Quantum Information* (Cambridge University Press, Cambridge, 2000).
[2] R. Jozsa and N. Linden, Proc. R Soc. London **459**, 2011 (2003).
[3] G. Vidal, Phys. Rev. Lett. **91**, 147902 (2003).
[4] D. Gottesman and I. Chuang, Nature **402**, 390 (1999).
[5] E. Knill and R. Laflamme, Phys. Rev. Lett. **81**, 5672 (1998).
[6] A. Datta, PhD thesis, 2008, e-print arXiv:0807.4490.
[7] J. Jones, Prog. Nucl. Magn. Reson. Spectrosc. **38**, 325 (2001).
[8] S. L. Braunstein, C. M. Caves, R. Jozsa, N. Linden, S. Popescu, and R. Schack, Phys. Rev. Lett. **83**, 1054 (1999).
[9] M. A. Nielsen, E. Knill, and R. Laflamme, Nature **396**, 52 (1998); L. M. K. Vandersypen *et al.*, *ibid.* **414**, 883 (2001).
[10] R. Raussendorf and H. J. Briegel, Phys. Rev. Lett. **86**, 5188 (2001); R. Raussendorf, D. E. Browne, and H. J. Briegel, Phys. Rev. A **68**, 022312 (2003).
[11] M. J. Bremner, C. Mora, and A. Winter, Phys. Rev. Lett. **102**, 190502 (2009); D. Gross, S. T. Flammia, and J. Eisert, *ibid.* **102**, 190501 (2009).
[12] D. Deutsch and R. Jozsa, Proc. R. Soc. London A **439**, 553 (1992).
[13] D. Collins, K. W. Kim, and W. C. Holton, Phys. Rev. A **58**, R1633 (1998).
[14] J. Anders, D. K. L. Oi, E. Kashefi, D. E. Browne, and E. Andersson, Phys. Rev. A **82**, 020301(R) (2010).
[15] C. H. Bennett, D. P. DiVincenzo, P. W. Shor, J. A. Smolin, B. M. Terhal, and W. K. Wootters, Phys. Rev. Lett. **87**, 077902 (2001).
[16] M. Horodecki, P. Horodecki, and R. Horodecki, Phys. Rev. A **60**, 1888 (1999).
[17] Y. S. Weinstein, Phys. Rev. A **79**, 052325 (2009).
[18] R. Chaves and L. Davidovich, Phys. Rev. A **82**, 052308 (2010).
[19] T. Morimae, Phys. Rev. A **81**, 060307(R) (2010).
[20] T. Morimae and J. Kahn, Phys. Rev. A **82**, 052314 (2010).
[21] J. Preskill, Proc. R. Soc. London **454**, 385 (1998).
[22] R. Raussendorf, J. Harrington, and K. Goyal, Ann. Phys. **321**, 2242 (2006).
[23] M. Hein, W. Dür, and H. J. Briegel, Phys. Rev. A **71**, 032350 (2005).
[24] D. Cavalcanti, R. Chaves, L. Aolita, L. Davidovich, and A. Acin, Phys. Rev. Lett. **103**, 030502 (2009); O. Gühne, F. Bodoky, and M. Blaauboer, Phys. Rev. A **78**, 060301(R) (2008); L. Aolita, D. Cavalcanti, R. Chaves, C. Dhara, L. Davidovich, and A. Acin, *ibid.* **82**, 032317 (2010).
[25] R. C. Drummond and M. O. Cunha, J. Phys. A **42**, 285308 (2009).
[26] Classically correlated quantum states are thus formed by the natural embedding of correlated classical random variables within a quantum mechanics framework, see [33] for more details. As such, these states are not only separable but also have zero discord [31].
[27] A. Montanaro, Inf. Process. Lett. **110**, 1110 (2010).
[28] W. K. Wootters, Phys. Rev. Lett. **80**, 2245 (1998).
[29] G. Vidal and R. F. Werner, Phys. Rev. A **65**, 032314 (2002).
[30] Bellow the 2/3 threshold, depicted by the horizontal dashed line in Fig. 1, a model of classical local-hidden variables is sufficient to reproduce all the correlations presented by the resource state, and thus also to achieve the obtained computation fidelity.
[31] H. Ollivier and W. H. Zurek, Phys. Rev. Lett. **88**, 017901 (2001).
[32] S. Luo, Phys. Rev. A **77**, 042303 (2008).
[33] M. Piani, S. Gharibian, G. Adesso, J. Calsamiglia, P. Horodecki, and A. Winter, Phys. Rev. Lett. **106**, 220403 (2011).
[34] A. Streltsov, H. Kampermann, and D. Bruss, Phys. Rev. Lett. **106**, 160401 (2011).
[35] P. Jorrand and M. Mhalla, IJFCS **14**, 797 (2003).
[36] E. Biham *et al.*, Theor. Comput. Sci. **320**, 15 (2004).
[37] M. S. Tame, R. Prevedel, M. Paternostro, P. Bohi, M. S. Kim, and A. Zeilinger, Phys. Rev. Lett. **98**, 140501 (2007); G. Vallone, G. Donati, N. Bruno, A. Chiuri, and P. Mataloni, Phys. Rev. A **81**, 050302 (2010); M. S. Tame and M. S. Kim, *ibid.* **82**, 030305(R) (2010).
[38] D. R. Simon, SIAM J. Comput. **26**, 1474 (1997).
[39] G. Engel *et al.*, Nature **446**, 782 (2007); T. Scholak, F. de Melo, T. Wellens, F. Mintert, and A. Buchleitner, Phys. Rev. E **83**, 021912 (2011).